

2356-24

Targeted Training Activity: ENSO-Monsoon in the Current and Future Climate

30 July - 10 August, 2012

ENSO-THE PAST AND FUTURE

SARACHIK Edward Stuart

*Joint Institute For the Study of the Atmosphere and Ocean, JISAO
University of Washington, 3737 Brooklyn Ave. NE, Box 355672
Seattle WA 98195-5672
U.S.A.*

ENSO-THE PAST AND FUTURE

E.S. Sarachik, University of Washington

a. THE DEPENDENCE OF ENSO ON THE CLIMATOLOGY

b. ENSO IN THE PAST

c. ENSO AND GLOBAL WARMING

a. THE DEPENDENCE OF ENSO ON THE CLIMATOLOGY

▶ **THE BASIC MEAN CLIMATOLOGICAL COLD TONGUE DETERMINES THE STRUCTURE OF THE WARM PHASE ANOMALY**

STRONGEST WARM PHASE SIMPLY FILLS IN THE COLD TONGUE

▶ **BASIC QUESTION: HOW DOES THE EAST-WEST TEMPERATURE GRADIENT INCREASE OR DECREASE**

THROUGHOUT TIME

IN THE FUTURE AS THE WORLD WARMS

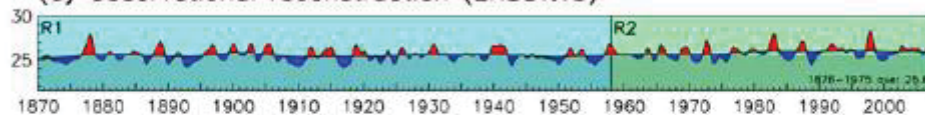
▶ **BASIC QUESTION: HOW DOES THE TROPICAL THERMOCLINE DEPTH CHANGE WITH TIME**

WHAT DOES THIS DEPTH DEPEND ON?

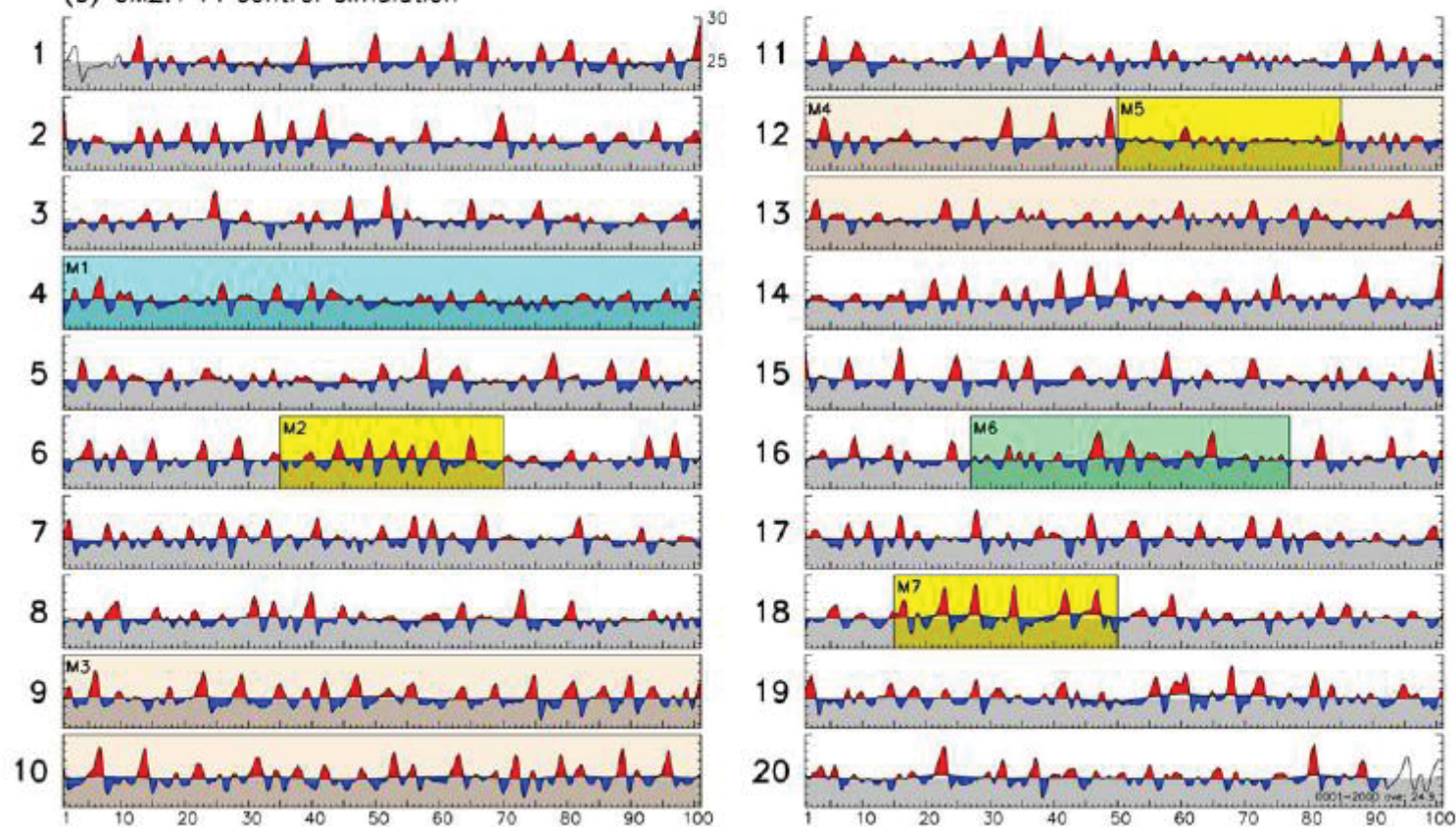
▶ **IS THE VARIABILITY OF ENSO SUCH THAT WE HAVE LONG ENOUGH RECORDS TO DISTINGUISH?**

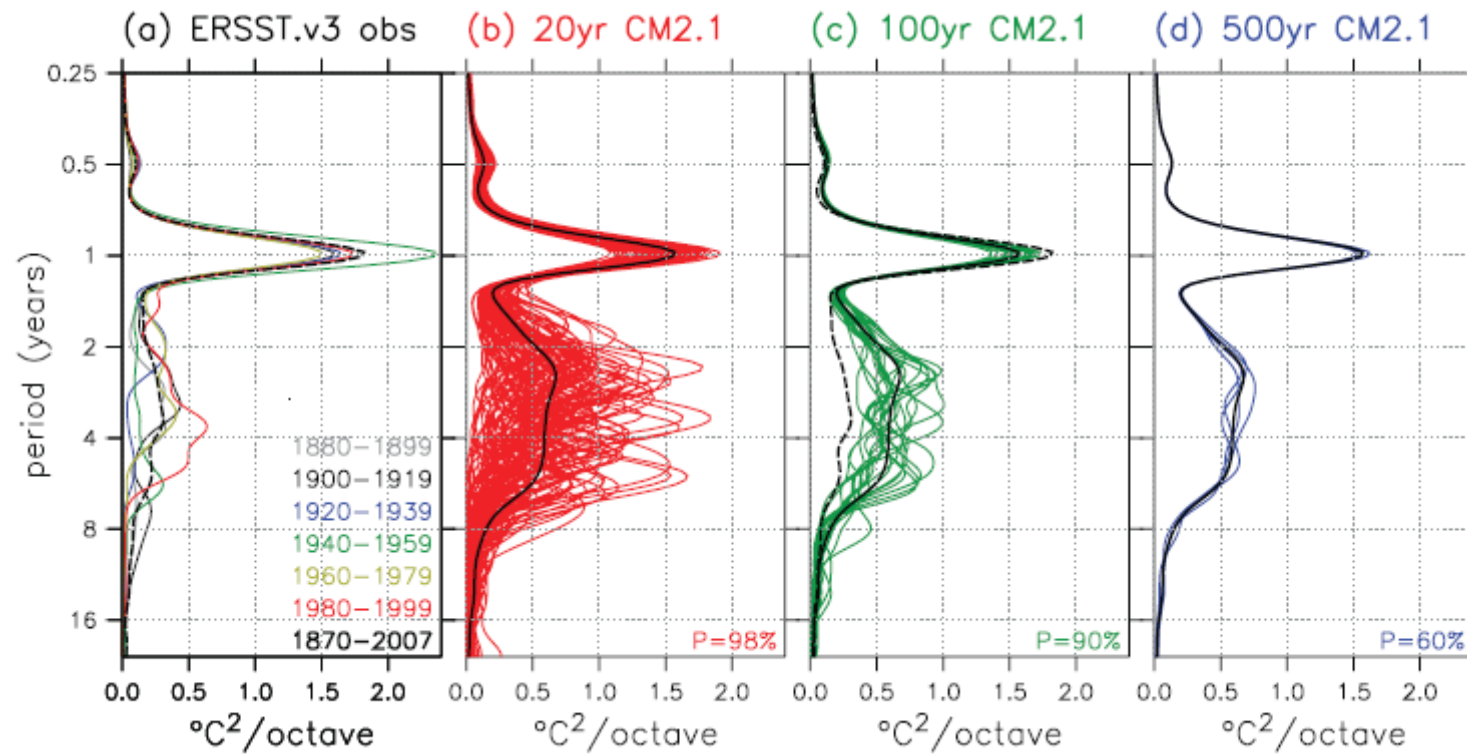
NINO3 SST ($^{\circ}\text{C}$):
running annual mean
& 20yr low-pass

(a) Observational reconstruction (ERSST.v3)

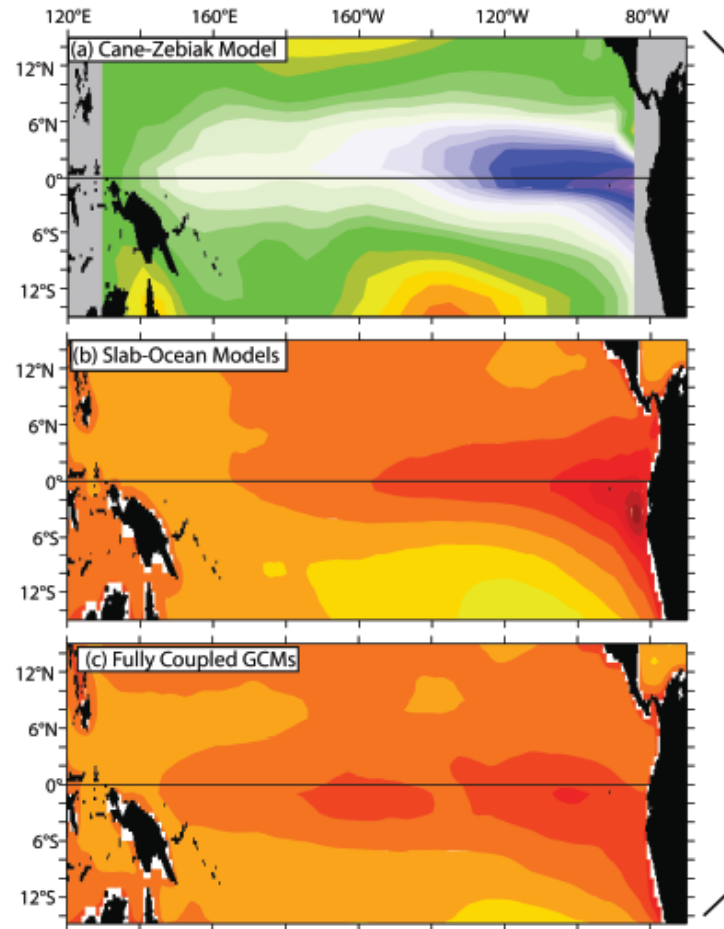


(b) CM2.1 PI control simulation

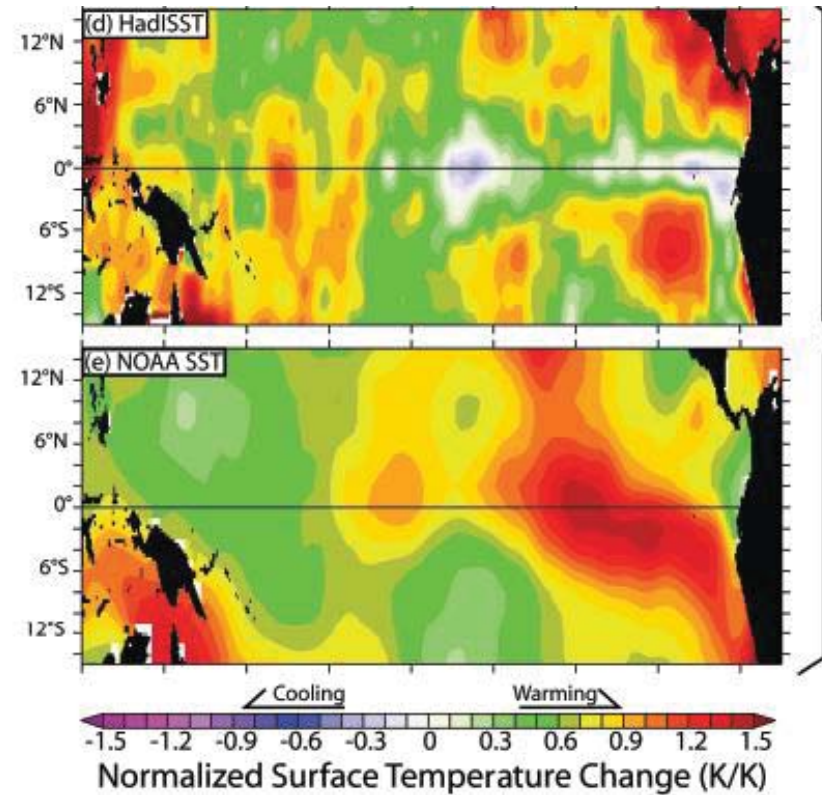




START BY LOOKING AT THE E-W TEMPERATURE GRADIENT ON THE EQUATOR:



MODEL RESPONSE IN WARMING CLIMATE



OBSERVATIONAL ESTIMATES
1880-2005 Linear Trend in Reconstructed Historical SST

Vecchi, Clement, Soden, 2008

► **MODELS GIVE DIFFERENT RESULTS**

► **IT IS NOT CLEAR OBSERVATIONS CAN DISTINGUISH:**

Karnaskas et al, 2009

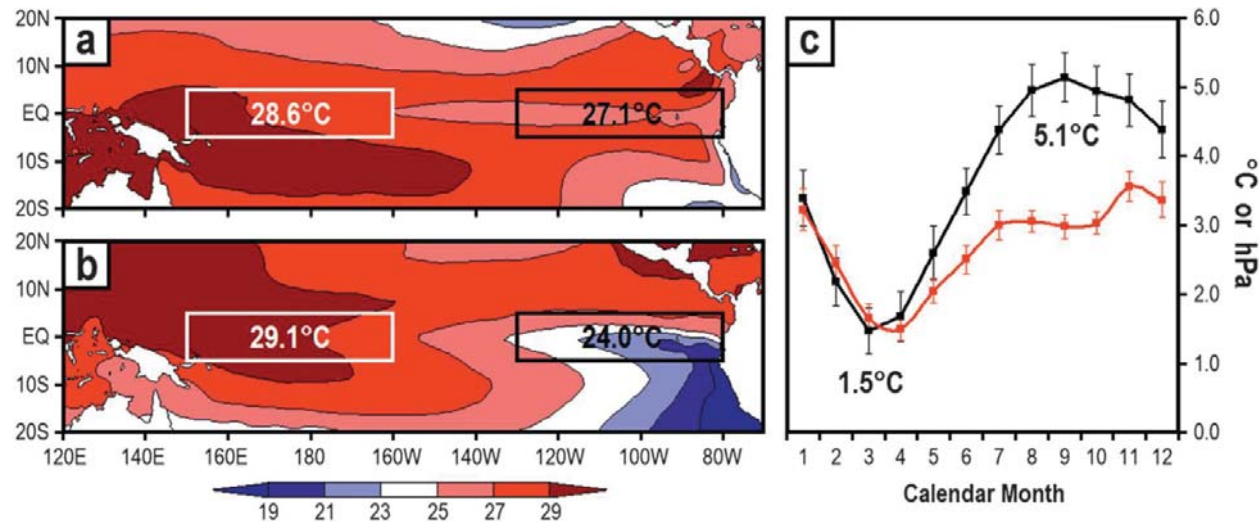


FIG. 1. Observed tropical Pacific SST (°C) in (a) March and (b) September averaged over the modern satellite era (1982–2007) from the NOAA Optimal Interpolation (OI) SST version 2 dataset (Reynolds et al. 2002). The white (black) rectangles represent the western (eastern) equatorial Pacific. (c) Observed annual cycle of equatorial Pacific Δ_x SST (black, °C) and Δ_x SLP (HadSLP2; red, hPa) averaged over the same period. Error bars represent ± 2 standard errors of the mean.

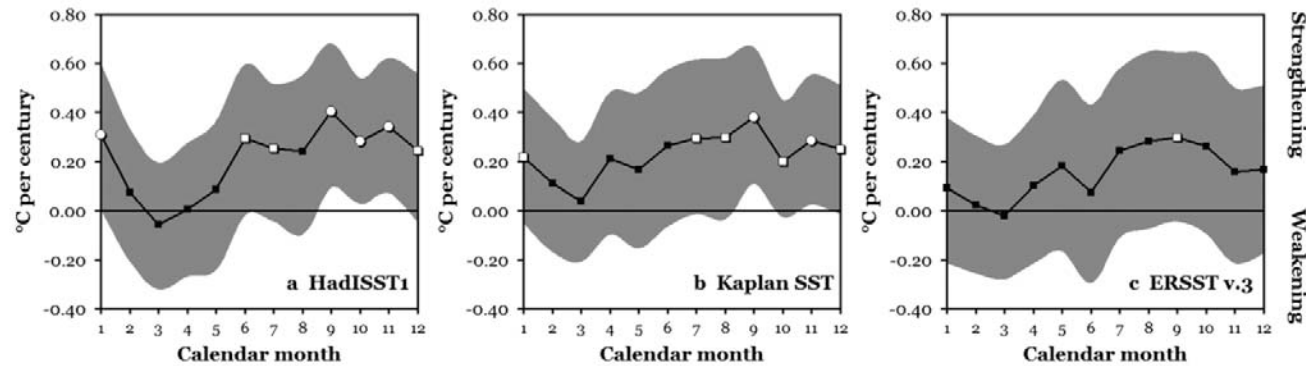


FIG. 2. Trends of observed equatorial Pacific Δ_x SST (°C century⁻¹) from 1880 to 2005 as a function of calendar month from (a) HadISST1, (b) Kaplan SST, and (c) NOAA ERSST v3. Gray shading denotes 95% confidence intervals based on the nonparametric Sen median slope method. White circles (squares) represent trends significant at the 5% (10%) level based on the nonparametric Mann-Kendall test.

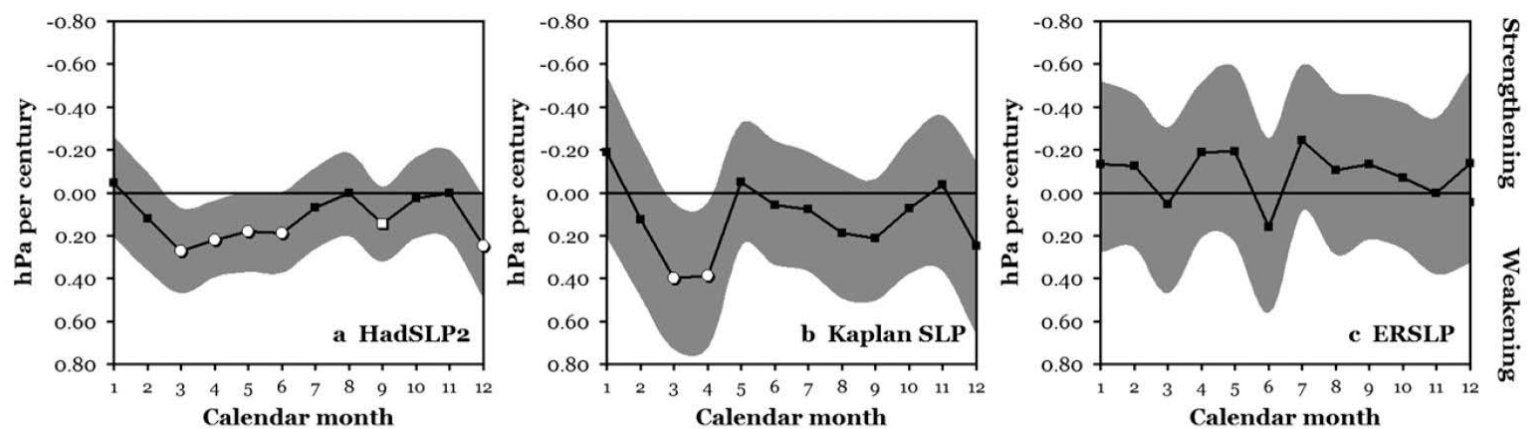


FIG. 4. Same as Fig. 2, but for $\Delta_x \text{SLP}$ based on (a) HadSLP2, (b) Kaplan SLP, and (c) NOAA ERSLP. Note the vertical scale is inverted so that up corresponds to a strengthening of the SLP gradient ($\Delta_x \text{SST}$), and vice versa.

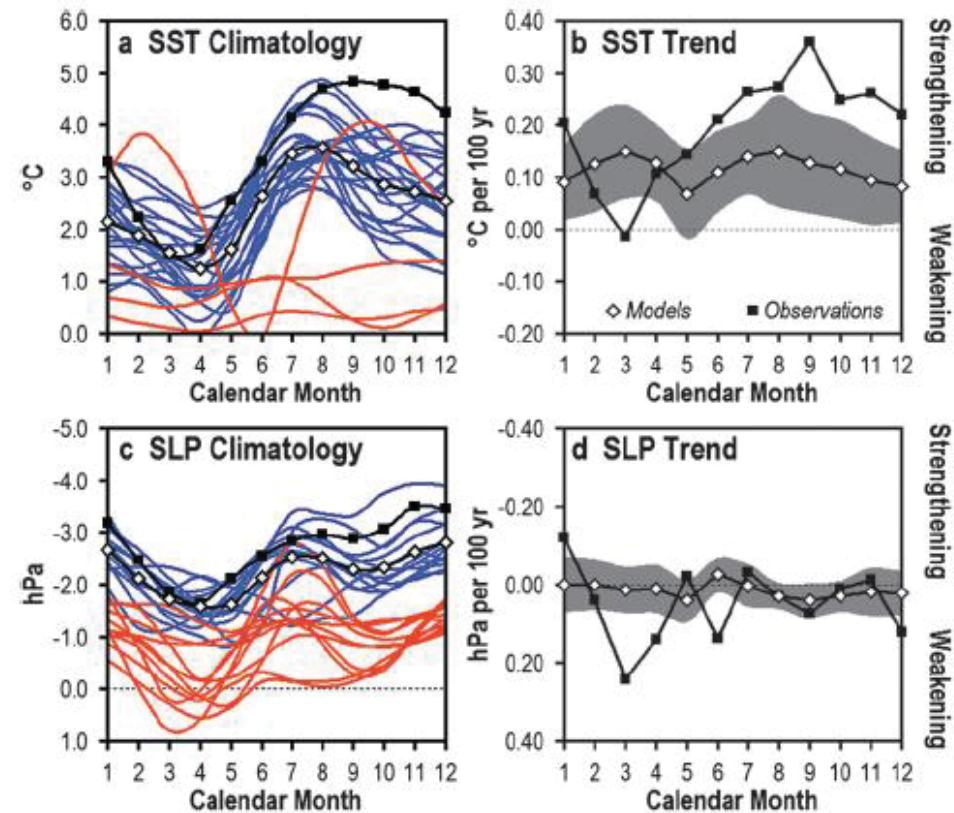
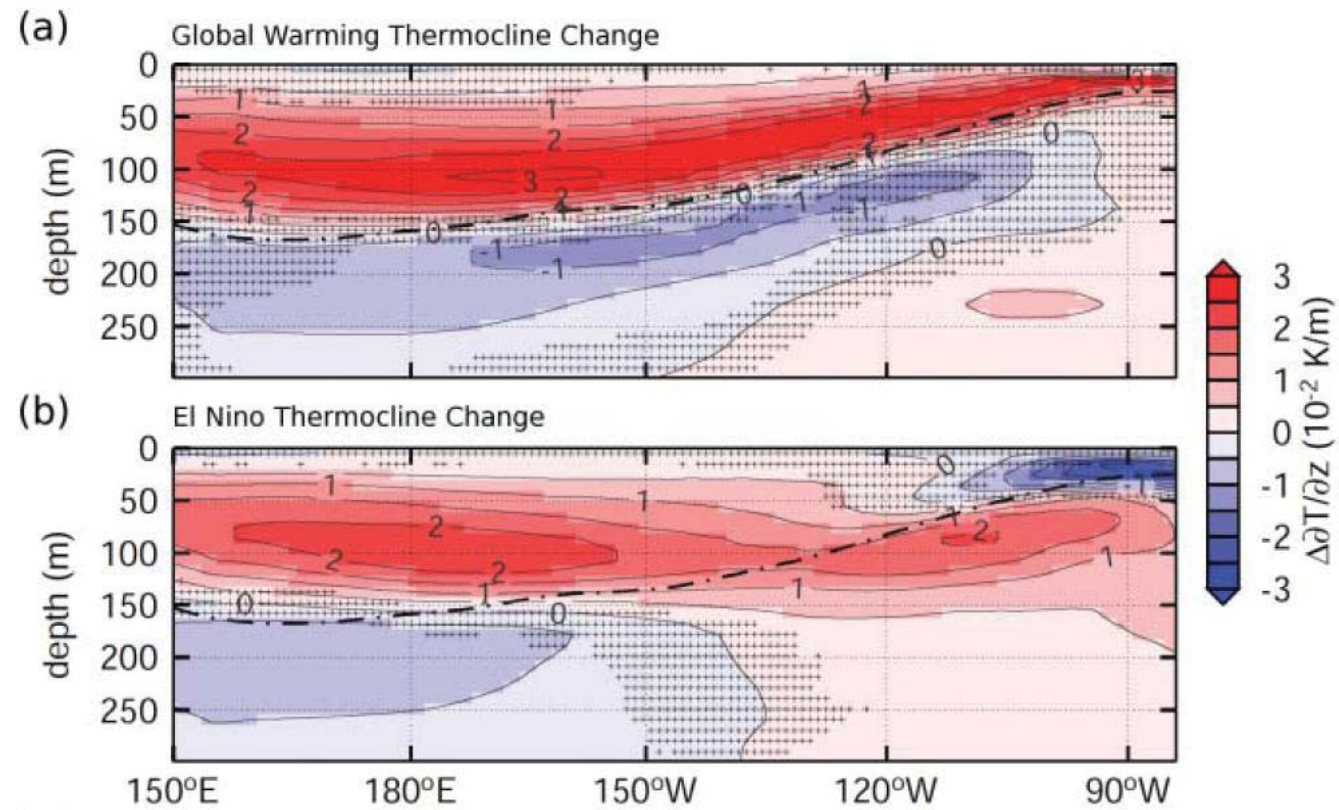


FIG. 5. Annual cycle of equatorial Pacific (a) $\Delta_x \text{SST}$ and (c) $\Delta_x \text{SLP}$ computed over the "Climate of the Twentieth Century" experiments for 24 coupled GCMs. A subset of models is easily distinguishable as having an unrealistic annual mean and/or seasonality of $\Delta_x \text{SST}$ (red lines). The black line with open markers represents the multimodel ensemble mean of the blue lines. The black line with closed markers represents the observations (multidataset mean, 1880–2005). Multimodel ensemble mean (blue models only; open markers) and observed (multidataset mean; closed markers) linear trend in (b) $\Delta_x \text{SST}$ and (d) $\Delta_x \text{SLP}$ as a function of calendar month. Gray shading represents ± 2 standard errors of the multimodel ensemble mean trends.

Models



DiNezio et al, 2010

b. ENSO IN THE PAST

WHY ARE WE INTERESTED IN PAST ENSO?

▶ **TO EXAMINE PAST RELATIONS BETWEEN ENSO AND MEAN CLIMATE**

▶ **TO SEE HOW ENSO RESPONDS TO DIFFERENT TYPES OF FORCING THAT EXISTED IN THE PAST**

VOLCANOES

DIFFERENT LEVELS OF GREENHOUSE GASES

DIFFERENT AEROSOL BURDENS

DIFFERENT DEEP OCEAN CIRCULATIONS

DIFFERENT EFFECTIVE SOLAR FORCING

▶ **TO UNDERSTAND THE FORCING OF MID-LATITUDES BY THE TROPICS WHEN THE GENERAL CIRCULATION OF THE EARTH WAS DIFFERENT**

▶ **TO PROVIDE PAST DATA FOR INITIALIZING AND VALIDATING ENSO FORECASTS**

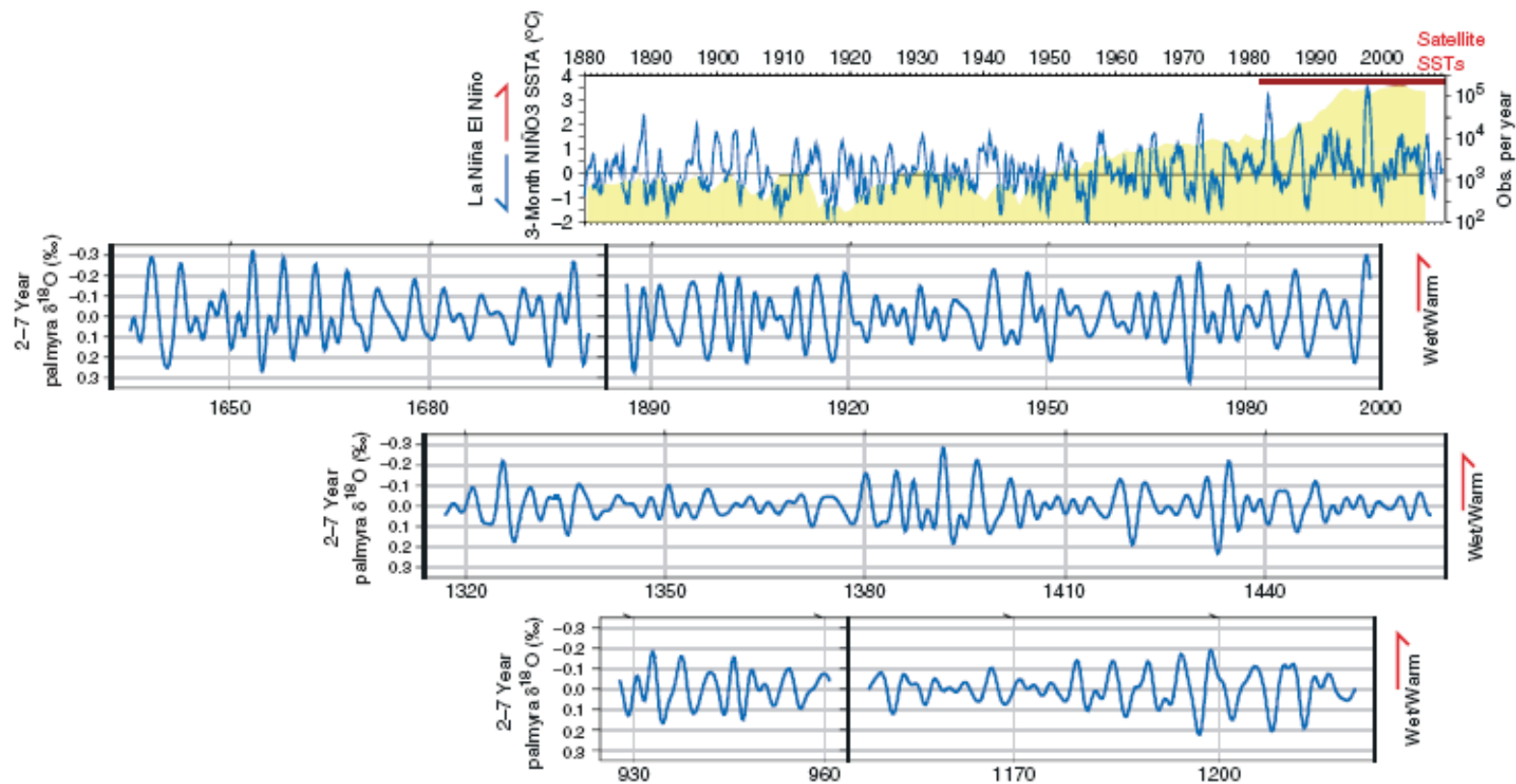


FIGURE 2 | Instrumental and coral-based records of El Niño/La Niña. Upper time series shows the monthly Niño-3.4 sea surface temperature (SST) anomaly index from Ref 12 (blue line, left scale), the logarithm of the number of SST observations per year in the Niño-3.4 region based on Ref 11 (yellow shading, right scale), and the era in which satellite estimates of SST are available (red horizontal line). Lower time series show the 2–7-year filtered ratio of Oxygen-18 to Oxygen-16 isotope concentrations from corals taken from Palmyra Island—with positive values indicating warmer, wetter conditions associated with El Niño—after Ref 13. See Figure 1(a,b) for location of Palmyra Island and the Niño-3.4 region. (Lower panels are reprinted with permission from Ref 13. Macmillan Publishers Ltd. Copyright 2003).

THERE ARE INDICATIONS THAT ENSO WAS ABSENT (OR WEAKENED) DURING THE EARLY HOLOCENE AND STARTING PICKING UP DURING THE MID-HOLOCENE.

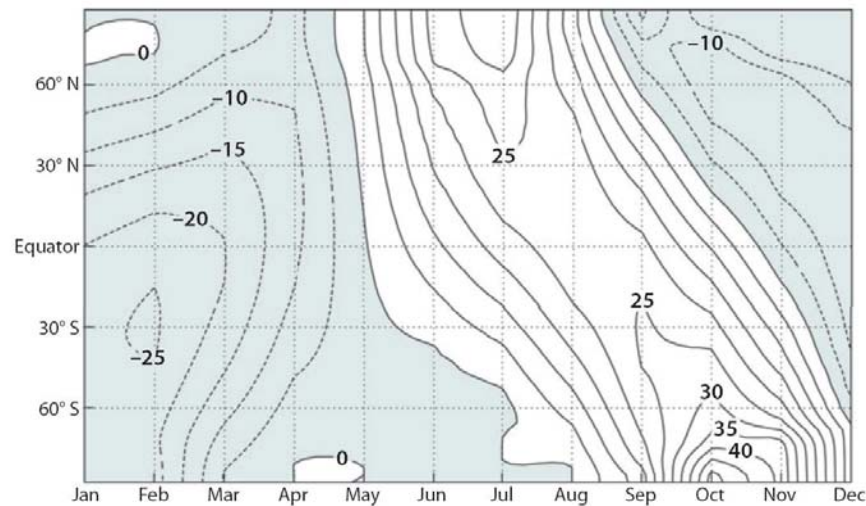


Figure 6

Top-of-atmosphere changes to insolation during the mid-Holocene (6000 years ago). The contour interval is 5 W m^{-2} , and positive values (*unshaded*) are directed toward the earth. The peak anomalies, which can exceed 30 W m^{-2} in the polar regions, are substantially larger than comparable radiative forcing from today's enhanced greenhouse effect (on the order of a few watts per square meters).

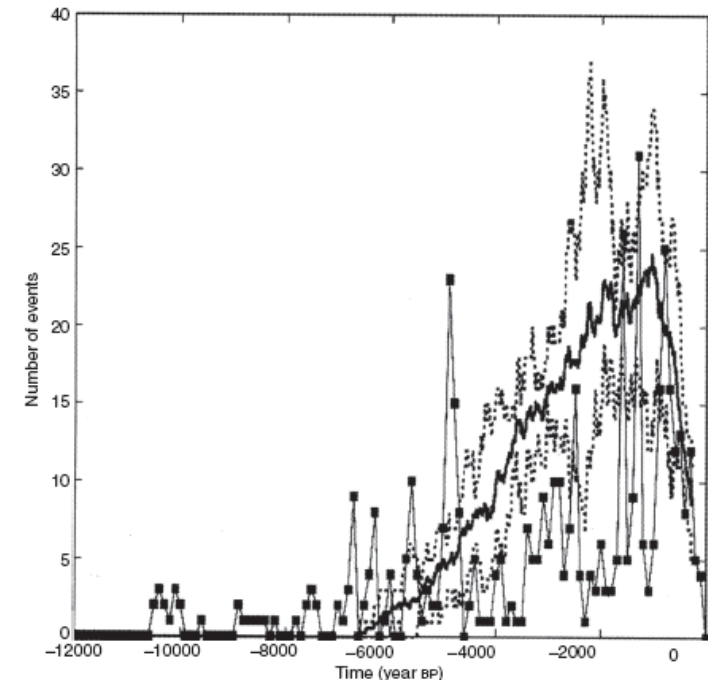


Figure 9.2. Number of warm ENSO events in 100-year windows. The black line with squares represents proxy data from a lake in Ecuador (Moy *et al.*, 2002). Warm ENSO events are defined as light-colored strata in the sediment record, which reflect pluvial episodes during large El Niño (warm) events. The solid line shows the ensemble mean of seven simulations with the Zebiak–Cane model forced by the orbital variations of the last 12 000 years. The dotted lines show the minimum and maximum values over the ensemble. Warm ENSO events are defined in the model as years in which the DJF SST anomaly in the NINO 3 region (5°N – 5°S , 90°W – 150°W) exceeds 3°C . This event index corresponds to the middle of the rainy season in coastal South America during which large SST anomalies associated with ENSO events are capable of causing the ITCZ to move equatorward and bring large precipitation anomalies to the region. (From Cane *et al.*, 2006.)

THE PROPOSED EXPLANATION IS THAT THE SOLAR RADIATION WAS HIGHER IN (BOREAL) LATE SUMMER AND FALL AND LESS IN (BOREAL) WINTER. THIS KEEPS THE ITCZ FAR FROM THE EQUATOR AND DOESN'T ALLOW THE CONVERGENCE FROM REACHING THE EQUATOR SO THE WARM ENSO EVENTS CAN'T GROW.

c. ENSO AND GLOBAL WARMING

THERE ARE TWO CONFLICTING ARGUMENTS FOR THE E-W TEMPERATURE DIFFERENCE UNDER GLOBAL WARMING:

1. THE WEST WARMS MORE THAN THE EAST BECAUSE THE UPWELLING THAT KEEPS THE EAST COLD HAS MORE THERMAL INERTIA AND THE EAST WARMS MORE SLOWLY.

2. PRECIPITATION INCREASES SLOWER THAN BOUNDARY LAYER HUMIDITY SO

$$P = M_c q_M$$

AND THEREFORE M_c MUST DECREASE. SINCE THE DRIVING FOR THE CIRCULATION DECREASES, THE CIRCULATION ITSELF MUST DECREASE WHICH IMPLIES THE E-W TEMPERATURE DIFFERENCE AND THE E-W PRESSURE DECREASES.

[DOES M_c DECREASING REALLY IMPLY \bar{M} DECREASES?]

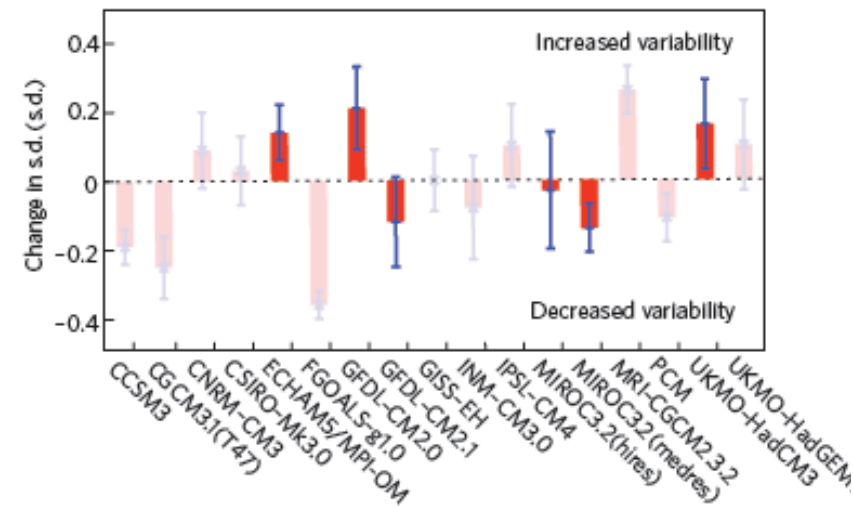


Figure 3 | Projected changes in the amplitude of ENSO variability, as a response to global warming, from the CMIP3 models^{8,9}. The measure is derived from the interannual standard deviation (s.d.) of a mean sea-level-pressure index, which is related to the strength of the Southern Oscillation variations. Positive changes indicate a strengthening of ENSO, and negative changes indicate a weakening. Statistical significance is assessed by the size of the blue bars, and the bars indicated in bold colours are from those CMIP3 CGCMs that are judged to have the best simulation of present-day ENSO characteristics and feedbacks.

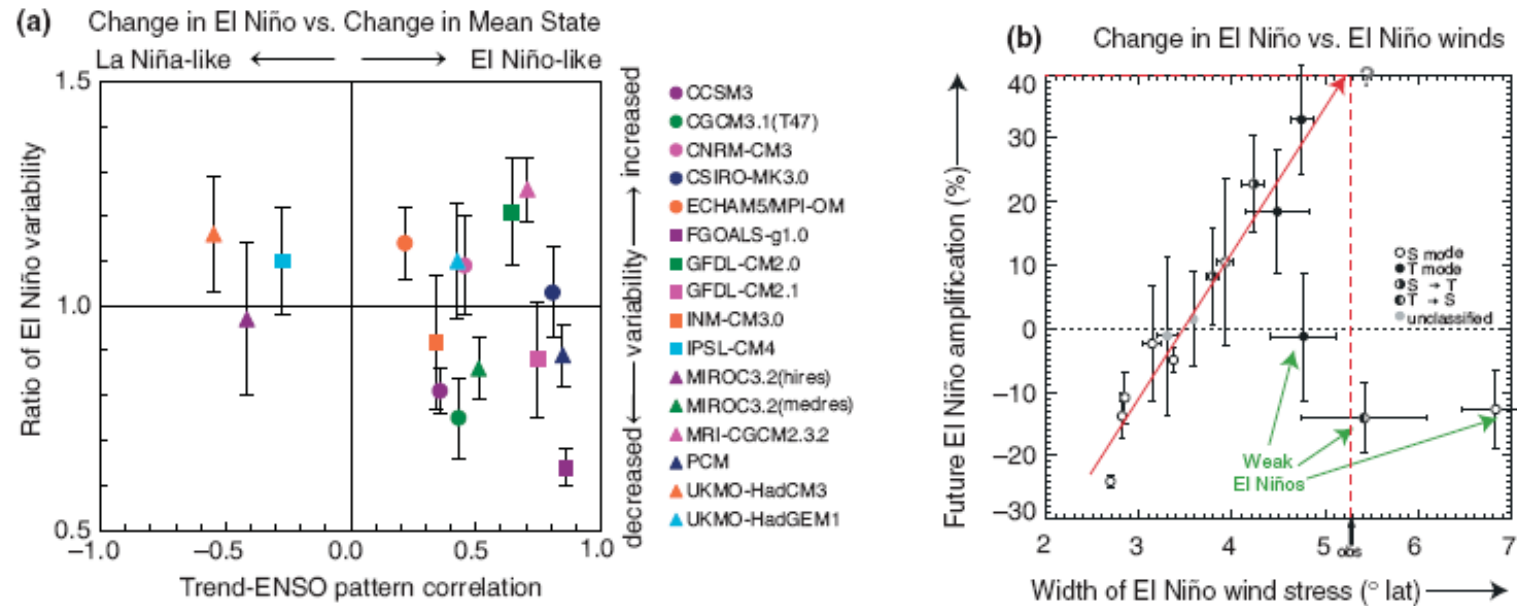


FIGURE 5 | Twenty-first century projected changes in El Niño characteristics. (a) Multimodel projections of changes in tropical Pacific sea level pressure mean state (horizontal axis) versus change in El Niño sea surface temperature variability (vertical axis); the 'mean state' change in each model is characterized by its similarity to the pattern of El Niño variability. Changes in mean state and El Niño are computed by comparing the end of the 21st century projections with the end of the 20th century from the analysis of Ref 32. (b) Change in El Niño amplitude (vertical axis) versus the meridional (north–south) width of the preindustrial near-equatorial westerly wind anomalies associated with El Niño, in response to increasing levels of atmospheric CO₂, from the CMIP3 ensemble of global climate models; different symbols indicate character of model response as characterized in Ref 58. The three models highlighted by green Ref 47 arrows have 20th century El Niño variations that are much weaker than the observed and are considered less reliable. (Left panel adapted with permission from Ref 48. Copyright 2009; Right panel adapted with permission from Ref 60. Copyright 2006 American Meteorological Society).